The 2005 Ilan earthquake doublet and seismic crisis in northeastern Taiwan: evidence for dyke intrusion associated with on-land propagation of the Okinawa Trough

Kuang-Yin Lai,[1] Yue-Gau Chen,[1] Yih-Min Wu,[1] Jean-Philippe Avouac,[2] Yu-Ting Kuo,[1] Yu Wang,[2] Chien-Hsin Chang[3] and Kuan-Chuan Lin[1,3]

[1]*Department of Geosciences, National Taiwan University, No. 1, Section 4th, Roosevelt Road, Taipei 106, Taiwan. E-mail: d92224003@ntu.edu.tw*
[2]*Division of Geological and Planetary Sciences, California Institute of Technology, Pasadena, CA 91125, USA*
[3]*Seismological Observation Center of the Central Weather Bureau, Taipei 100, Taiwan*

SUMMARY

Northern Taiwan underwent mountain building in the early stage of the Taiwan orogeny but is currently subjected to post-collisional crustal extension. It may be related to gravitational collapse or to the rifting of the Okinawa Trough, which lies offshore northeastern Taiwan. The Ilan Plain, northeastern Taiwan, which is bounded by the normal fault systems and filled up with thick Pliocene–Pleistocene sedimentary sequences, formed under such an extension environment. Over there on 2005 March 5 two earthquakes with about the same magnitude ($M_L = 5.9$) occurred within 68 s and produced intense aftershocks activity according to the records of Central Weather Bureau Seismic Network of Taiwan. We relocated the earthquake sequence by the three-dimension earthquake location algorithm with the newly published 3-D Vp and Vp/Vs velocity model, and determined the first-polarity focal mechanisms of the earthquake doublet. One major cluster of aftershocks which trends E–W and dips steeply to the south can be identified and picked up as a potential fault plane. The focal mechanisms of the two main shocks are both classified as normal type by first-polarity but strike-slip by centroid moment tensor inversion; however two methods both yield consistent E–W strike. Static coseismic deformation was additionally determined from Global Positioning System (GPS) daily solutions at a set of continuous GPS stations and from strong-motion seismographs. These data show NW–SE extension at high angle to the fault plane, which cannot be explained from a simple strike-slip double-couple mechanism. On the other hand, the small vertical displacements and steep fault plane cannot be explained from a simple normal event as well. We present from elastic dislocation modelling that the geodetic data are best explained by significant component of tensile source with centimetre-scale of opening on a 15-km-long fault extending from 1 to 13 km depth. We therefore interpret the crisis as the result of dyke intrusion at the very tip of the Okinawa Trough, which is reasonably driven by backarc spreading.

Key words: Seismicity and tectonics; Backarc basin processes; Dynamics: seismotectonics; Neotectonics; Kinematics of crustal and mantle deformation; Crustal structure.

1 INTRODUCTION

Taiwan is located at an active plate boundary where an arc-continent collision has been acting between the Eurasian Plate and the northward subducting Philippine Sea Plate since late Miocene (Ho 1986, 1988; Teng 1990; Yu *et al.* 1997, Fig. 1a). On the basis of the orogenic evolution of the southward-migrating collision, the northern Taiwan has undergone the mountain building in the early stage, but is subjected to post-collision crustal extension since the Pleis-

tocene (Suppe 1984; Lee & Wang 1988; Teng 1996). To the east of the northeastern Taiwan the NE–SW trending Okinawa Trough behind the Ryukyu Arc is an actively rifting backarc basin, which is believed being accelerated by the southward migration of the collision in Taiwan. According to the topography, westernmost tip of the trough has pierced into northeastern Taiwan (Suppe 1984; Letouzey & Kimura 1986; Yeh *et al.* 1989; Liu 1995; Sibuet *et al.* 1998, Fig. 1b). The Quaternary volcanism in the northern Taiwan may also triggered by such a recent tectonic evolution
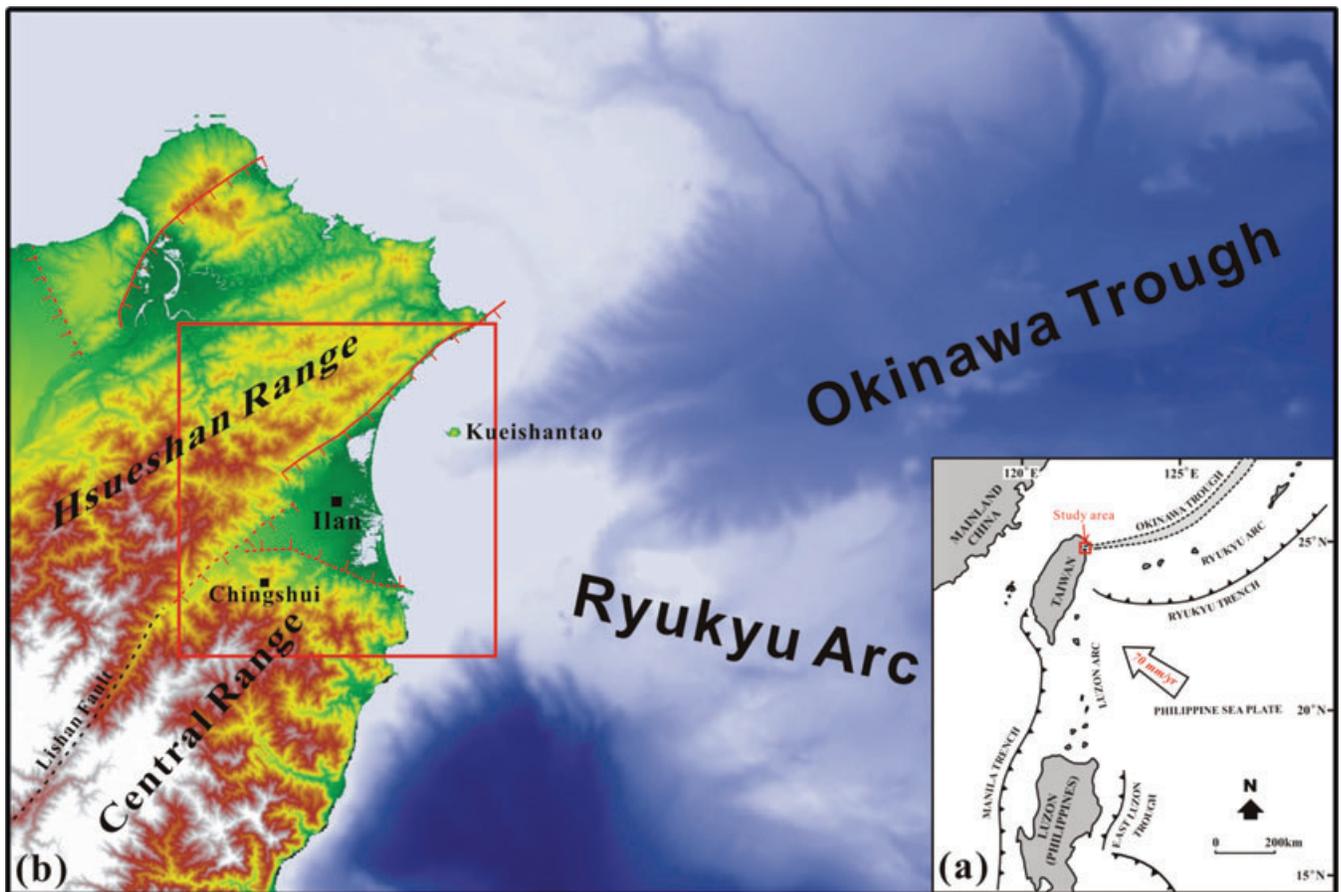
Figure 1. (a) Current tectonic environments of Taiwan, where the arc-continent collision has occurred since late Miocene and is still on-going based on that the Philippine Sea plate is moving northwestward with a speed of 70 mm yr^{-1} (Ho 1986, 1988; Teng 1990; Yu *et al.* 1997). (b) Map of northeastern Taiwan and offshore showing major normal faults and topographic relationship between Okinawa Trough and Ilan Plain. Ilan is the major city in Ilan Plain. Kueishantao is an active volcanic island (Chen *et al.* 1995; Wang *et al.* 1999; Chung *et al.* 2000; Chen *et al.* 2001). Chingshui is the largest geothermal area in Taiwan (Tseng 1978; Hsiao & Chiang 1979; Tong *et al.* 2008). Lishan Fault is one of the collision sutures of Taiwan (Shyu *et al.* 2005a). Red square shows the study area.

(Chen *et al.* 1995; Teng 1996; Wang *et al.* 1999; Chung *et al.* 2000).

The triangle-shaped Ilan Plain is bounded by the slaty Hsuehshan Range and the northern end of the metamorphic Central Range in the north and south, respectively (Fig. 1b). To its western apex the basin is closed and two above geologic entities merge into a fault, namely Lishan, one of the collision sutures of the disarticulation model of Taiwan (Shyu *et al.* 2005a, Fig. 1b). Based on the geophysical data, the depth of alluvial sediments in the Ilan Plain is about 1700 m in the deposition centre and the floor of the basin is composed of complex rock units (Chiang 1976; Yu & Tsai 1979). Geomophologically the Ilan Plain has been proposed as bounded by two normal fault systems on the north and south along the mountain front (Shyu *et al.* 2005b, Fig. 1b). The Global Positioning System (GPS) data clearly show NW–SE extension across the Ilan Plain (Yu *et al.* 1997; Hsu 1999; Ho 2007). Other geological and geophysical studies also indicated the extension of the southwestern Okinawa Trough has influenced the Ilan Plain (Tsai *et al.* 1975; Chiang 1976; Sheu 1987; Yeh *et al.* 1989; Liu 1995; Hsu *et al.* 1996). However, the field evidence of active faulting and the detailed crustal structures of both northern and southern normal faulting systems have not been clearly understood yet. Therefore, where the major seismogenic fault is potentially generating large earthquakes and what the acting

behaviour is are still enigma up to date. The rapid sediment accumulation in the Ilan Basin has been attributed to the active fault systems mentioned above, and it is still lacking evidence to exactly identify where they are. To tackle this problem seismological method may be another alternative by taking account of the abundant seismic activities in Ilan area. An earthquake doublet ($M_L = 5.9$) occurred within 68 s on 2005 March 5 (UT) at focal depths of 6.4 km and 7.0 km. The epicentres were located on-land at 24.65°N, 121.84°E and 24.65°N, 121.80°E close to the coastline of Ilan Plain according to the report of Central Weather Bureau (CWB) of Taiwan. The focal solutions of Harvard CMT and the Broadband Array in Taiwan Seismology (BATS) CMT are consistent and both indicate strike-slip motion dominated (Table 1). After the main shocks, hundreds of aftershocks occurred between March 5 and 17 (Fig. 2). Although the background seismicity is high in the Ilan area, barely earthquakes with magnitude larger than 6.0 even 5.0 were observed in the past 15 yr (Wu *et al.* 2008a) and the fault activity was also absent on record. The on-land earthquakes have the better data quality than those of offshore ones; therefore, the 2005 Ilan earthquake doublet and associated aftershocks provide a rare opportunity to explore the seismogenic structures underneath thick sedimentary sequence. In this study, we aim at acquiring the coseismic deformation by analysing relevant seismic data of this earthquake doublet event

Table 1. Source parameters of main shocks.

No.	Origin Time, UT (yr/month/d/hr:min)	Lon. (°E)	Lat. (°N)	Depth (km)	Mag.	Strike(1)	Dip(1)	Rake(1)	Strike(2)	Dip(2)	Rake(2)	CLVD (per cent)
[a]1	2005/03/05/19:06	121.81	24.70	12.00	M_W5.7	264.0	68.0	−26.0	4.0	66.0	−156.0	56
[a]2	2005/03/05/19:08	121.79	24.70	12.00	M_W5.7	261.0	77.0	−29.0	358.0	62.0	−165.0	53
[b]1	2005/03/05/19:06	121.85	24.67	19.00	M_W5.5	270.0	66.0	−10.0	5.0	81.0	−156.0	10
[b]2	2005/03/05/19:07	121.84	24.67	19.00	M_W5.5	266.0	81.0	−19	359.0	71.0	−171.0	18
[c]1	2005/03/05/19:06	121.83	24.67	7.38	M_L5.9	40.0	30.0	−105.0	237.0	61.0	−82.0	NIL
[c]2	2005/03/05/19:08	121.81	24.67	6.71	M_L5.9	30.0	47.0	−125.0	256.0	53.0	−58.0	NIL

Notes: (1) and (2) are revealed fault plane 1 and fault plane 2, respectively. CLVD (per cent) is the percentage of compensated linear vector dipole component.
[a]Harvard CMT solution.
[b]BATS CMT solution.
[c]First-polarity solution (this study).
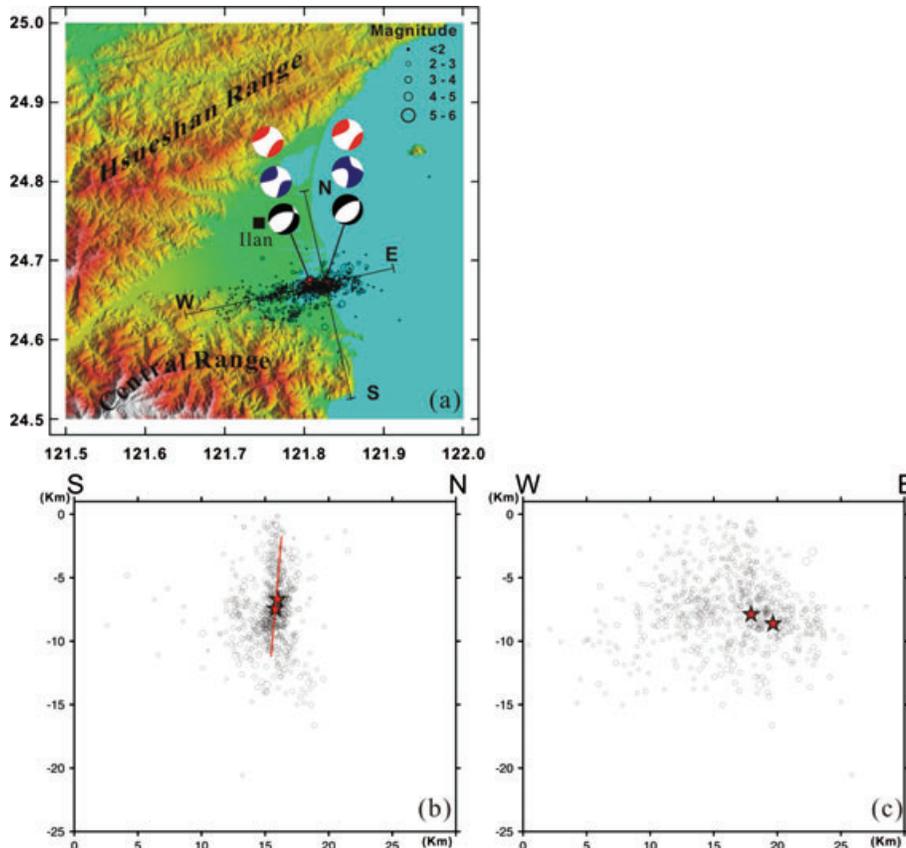
Figure 2. (a) The distribution of relocated epicentres of the two main shocks and associated aftershocks of the 2005 Ilan earthquakes in northeastern Taiwan and the lower-hemisphere focal mechanisms of two main shocks M_L = 5.9 (Table 1). Red, blue and black represent the Harvard CMT, BATS CMT and first-polarity focal mechanisms, respectively. Base map is shaded relief topographic map of the study area derived from 40 m DEM (see location in Fig. 1b). (b) N–S and (c) E–W cross-sections of projected hypocentres showing one major cluster can be identified and picked up as a potential fault plane, dipping south with steep angle.

2 DATA ACQUISITION AND PROCESSING

In this study, we employed two sets of seismic data. One is the phase data from the catalogs of the Central Weather Bureau Seismic Network (CWBSN) containing a total of 71 telemetered stations with three-component S-13 Teledyne Geotech seismometers (Wu *et al.*

to identify the 2005 seismogenic structure and further proposing a model to explain the structure which is responsible to the development of the Ilan Plain.

2008a). The other is strong motion records from the Taiwan Strong Motion Instrumentation Program (TSMIP) consisting of over 700 digital accelerographs on free-field sites (Shin *et al.* 2003). Moreover we also used the daily solutions from the newly established continuous GPS data of Taiwan Continuous GPS Array established by CWB in Ilan area.From the catalogs of the CWBSN, 664 earthquakes from 2005 March 5–17 (UT) were selected for earthquakes relocation, in which the double main shocks are further determined their focal mechanisms by analysing the first *P*-wave polarities. The selection was based on the following criteria: (i) using 3 d and 5 km as parameter of time and spatial in method of double-link cluster analysis (Wu & Chiao 2006; Wu & Chen 2007; Wu *et al.* 2008b),

which is similar to the single-link cluster analysis (Davis & Frohlich 1991); (ii) recorded by at least six stations with clear *P* or *S* arrivals. Because the Ilan Plain is situated along the suture zone, the crustal velocity is rather heterogeneous for seismic studies. To improve the location accuracy the three-dimension earthquake location algorithm (Thurber & Eberhart-Phillips 1999) with stations corrections is adopted with the newly published 3-D Vp and Vp/Vs velocity model derived from the local dense arrays of CWBSN and TSMIP (Wu *et al.* 2003; Wu *et al.* 2007). Besides of the CWBSN data, over 60 strong motion records from TSMIP stations in the study area are further incorporated into focal mechanism determination (Wu *et al.* 2008c) and earthquake location (Wu *et al.* 2008a). Due to the high station density in the study area, the estimated error of the relative distance of relocated hypocentres should be statistically less than 300 m (Wu *et al.* 2003, 2008a), which is good enough to define the geometry of the seismicity clusters.

The TSMIP stations with digital recording systems and accelerometers also provide us the digital strong-motion records, containing the near-source strong-motion waveforms. The velocity and displacement of the station site itself in a large earthquake can be directly retrieved by integrations of the acceleration data if permanent displacement occurs at the site and the background noise is low enough. However, an applicable baseline correction is needed (Boore 2001; Boore *et al.* 2002). Several baseline correction methods for the digital strong-motion records had been proposed (e.g. Iwan *et al.* 1985; Chiu 1997). We used a baseline correction method with standardized procedure, proposed by Wu & Wu (2007) based on the pioneering work of Iwan *et al.* (1985) and Boore (2001), to derive the coseismic displacement from a digital strong-motion record (Fig. 3), successfully applied to faults modelling of 2003 Chengkung M_w 6.8 and 2006 Taitung M_w 6.1 earthquakes (Wu *et al.* 2006a,b). By this approach, we can retrieve individual coseismic displacement for the first main shock. On the other hand, the daily GPS measurements can provide the total displacement contributed by coseismic deformation of two main shocks and partly by post-seismic deformation. Unfortunately, we only obtained the sufficient coseismic displacement of the first main shock because the two main shocks temporally occurred too close to correctly find a baseline for the second main shock.

3 SEISMOGENIC STRUCTURE AND FAULT GEOMETRY FROM SEISMIC DATA

Shown in Fig. 2 are the relocated epicentres, hypocentres, and focal mechanisms of the main shocks. After relocation, the double main shocks are located at 24.670°N, 121.829°E and 24.672°N, 121.808°E with focal depths of 7.38 and 6.71 km, respectively. The second main shock took place 2 km to the west of the first one and shallower in depth. The relocated aftershocks are distributed as nearly an E–W zone (N075) in the southern Ilan Plain and most of the events occurred at focal depth shallower than 15 km (Fig. 2). The focal mechanisms of the double main shocks are both classified as normal type but different from the CMT solutions provided by either Harvard or BATS.

The profile projection and the 3-D image of the seismic sequence show the aftershocks distributed in a nearly vertical zone within 15 km, which is especially dense between 7 and 10 km in depth (Figs 2b and c). Base on spatial analysis, one major cluster could be identified and picked up as a potential fault plane, which is dipping toward south with steep angle (Fig. 2). As we assumed, the earth-
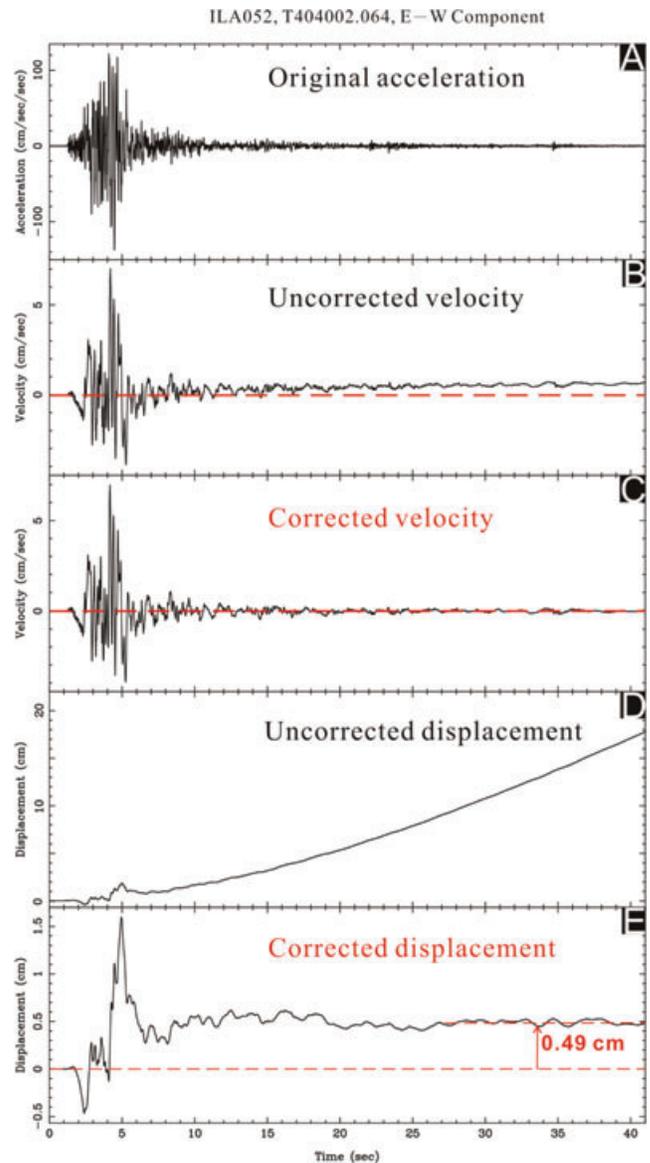
Figure 3. The procedures for converting a strong-motion record into a site displacement. The original accelerograph record (A) can be integrated into velocity and displacement (B/C and D/E) after baseline correction. In this record the displacement is 0.49 cm.

quake sequence usually occur along a rupture plane. In addition, the double main shocks occurred in association with the rupture plane. The above-mentioned fault plane therefore can be tentatively regarded as the seismogenic fault. Although we had difficulty in determining the behaviour of the seismogenic structure up to this step because of the conflict between different types of focal mechanism, the existence of seismogenic structure for the 2005 Ilan earthquake doublet underneath the Ilan Plain can be still confirmed.

4 COSEISMIC GROUND DISPLACEMENT FROM STRONG-MOTION RECORDS AND GPS MEASUREMENTS

The TSMIP stations are evenly distributed in Ilan Plain and neighbouring mountains in a rough density of a few kilometres. However,
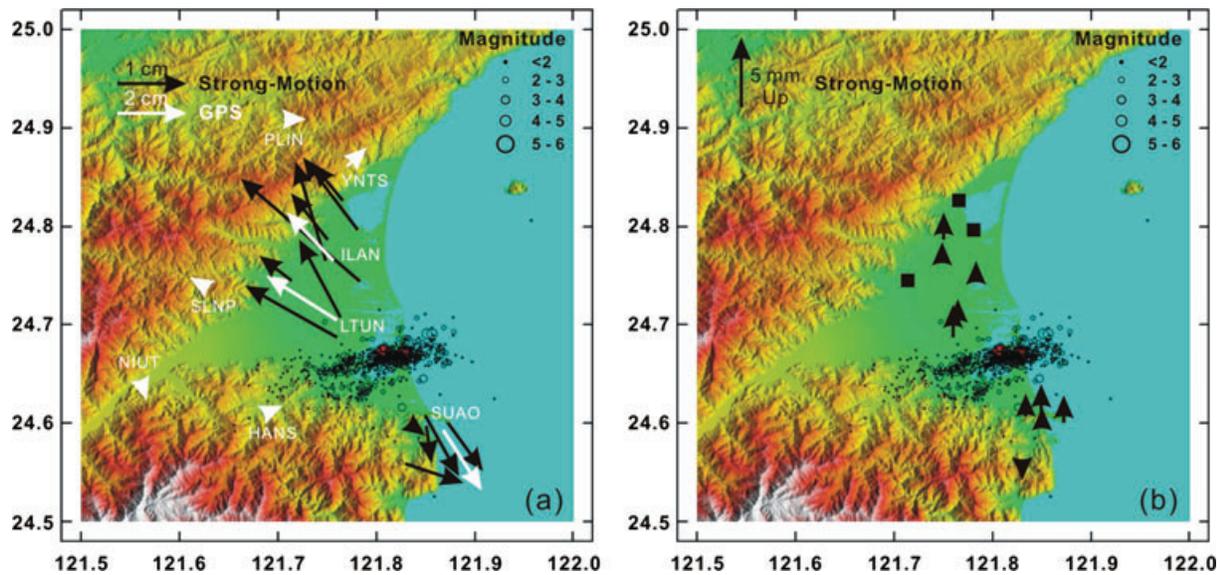
Figure 4. (a) Black arrows show coseismic horizontal displacement of the first main shock from strong-motion records and white arrows show coseismic horizontal displacements from daily solution continuous GPS data (Tables 2 and 3). (b) Black arrows show coseismic vertical displacement of the first main shock from strong-motion records. Black squares show no determinable coseismic vertical displacement of the first main (Table 2).

Table 2. 13 stations observed and modeled coseismic deformation of strong-motion records.

Station	Lat. (°)	Lon. (°)	Observed				Modelled			
			Vertical (cm)	North (cm)	East (cm)	H_Slip (cm)	Vertical (cm)	North (cm)	East (cm)	H_Slip (cm)
ILA003[a]	24.798	121.781	[b]0.00	1.04 ± 0.65	−0.79 ± 0.61	1.30 ± 0.89	0.16	0.49	−0.22	0.54
ILA004[a]	24.745	121.783	0.06 ± 0.27	1.48 ± 0.53	−1.71 ± 0.49	2.26 ± 0.72	0.39	0.82	−0.47	0.94
ILA008[a]	24.709	121.763	0.09 ± 0.16	1.12 ± 0.29	−0.59 ± 0.27	1.27 ± 0.40	0.67	1.08	−0.84	1.37
ILA027[a]	24.689	121.760	0.24 ± 0.19	0.74 ± 0.18	−1.32 ± 0.35	1.52 ± 0.39	0.85	1.09	−0.99	1.47
ILA031[c]	24.600	121.834	0.08 ± 0.09	−0.16 ± 0.06	0.22 ± 0.10	0.27 ± 0.12	0.15	−0.51	0.54	0.75
ILA036[a]	24.788	121.751	0.20 ± 0.04	0.67 ± 0.13	−0.53 ± 0.19	0.86 ± 0.23	0.18	0.59	−0.32	0.67
ILA037[a]	24.746	121.714	[b]0.00	0.36 ± 0.24	−0.47 ± 0.34	0.59 ± 0.42	0.28	0.74	−0.59	0.95
ILA049[a]	24.766	121.748	[b]0.00	1.42 ± 0.32	−0.43 ± 0.27	1.48 ± 0.42	0.25	0.72	−0.43	0.84
ILA052[c]	24.609	121.849	0.23 ± 0.08	−0.88 ± 0.02	0.49 ± 0.03	1.01 ± 0.04	0.19	−0.58	0.60	0.84
ILA068[c]	24.599	121.850	0.01 ± 0.09	−0.54 ± 0.27	0.07 ± 0.03	0.54 ± 0.27	0.18	−0.58	0.55	0.79
MND014[c]	24.603	121.872	0.20 ± 0.07	−0.70 ± 0.02	0.51 ± 0.05	0.86 ± 0.05	0.20	−0.61	0.58	0.84
TRB040[a]	24.827	121.766	[b]0.00	0.53 ± 0.19	−0.44 ± 0.27	0.69 ± 0.33	0.10	0.40	−0.18	0.43
TRB041[c]	24.561	121.828	−0.09 ± 0.06	−0.28 ± 0.14	0.84 ± 0.06	0.89 ± 0.15	0.10	−0.40	0.32	0.51

[a]Stations located in the north of the seismic cluster.
[b]Small acceleration.
[c]Stations located in the south of the seismic cluster.

some records of the first main shock were abandoned due to following factors: (i) mechanical collapse or tilt caused by the shock (especially located near the epicentre of the main shock); (ii) small acceleration and (iii) large standard error. Thereafter, we totally obtained the coseismic ground slips of the first main shock from 13 stations (Fig. 4; Table 2). For example, the corrected seismograms of the east-west component of ILA052 yield a coseismic eastward displacement of 0.49 cm with standard deviation of 0.03 cm (Fig. 3). The resulted horizontal components demonstrate that the stations located in the north of the cluster generally moved northwestward with values of 0.59–2.26 cm, while in the south the vectors turn southeastward with values of 0.27–1.01 cm (Fig. 4a; Table 2). The vertical components of most stations uplift with smaller values of <0.10 cm or less (Fig. 4b; Table 2). On the other hand, the daily solution of GPS measurements shows the opposite moving directions of horizontal displacements across the seismic cluster (Fig. 4a;

Table 3). The resulted GPS vertical displacements also show very small values, which are hardly to be solved since they usually smaller than daily error. Such a pattern is the same as revealed by strong-motion records but nearly double amounts of horizontal components by comparison of the data from GPS stations and their nearest strong motion stations (Fig. 4; Tables 2 and 3). The result of coseismic ground displacement indicates the southern and northern blocks moved away simultaneously in opposite direction with high angle to the fault plane, representing NW–SE extension.

5 DISLOCATION FAULT MODEL

Above-derived ground displacements are used to invert the fault model of the earthquake doublet event. The adopted method is the elastic dislocation model method, mainly modified from Okada

Table 3. Horizontal coseismic deformation from continuous GPS measurements with respect to Paisha, Penghu as stable Eurasian plate.

Station	Lat. (°)	Lon. (°)	Observed North (cm)	East (cm)	Slip (cm)	Modelled North (cm)	East (cm)	Slip (cm)
HANS	24.6095	121.6871	0.21 ± 0.03	0.48 ± 0.03	0.52 ± 0.04	0.56	0.61	0.83
ILAN	24.7640	121.7566	1.39 ± 0.05	-1.34 ± 0.05	1.94 ± 0.07	1.33	−0.89	1.60
LTUN	24.7000	121.7716	1.27 ± 0.03	-2.03 ± 0.03	2.39 ± 0.04	2.06	−2.18	3.00
NIUT	24.6348	121.5616	-0.05 ± 0.03	0.02 ± 0.03	0.05 ± 0.04	0.14	−0.13	0.19
PLIN	24.9336	121.7140	0.10 ± 0.03	0.03 ± 0.03	0.10 ± 0.04	0.36	−0.19	0.41
SLNP	24.7531	121.6356	0.32 ± 0.03	-0.53 ± 0.03	0.62 ± 0.04	0.73	−0.84	1.11
SUAO	24.5924	121.8671	-1.73 ± 0.07	1.11 ± 0.10	2.06 ± 0.12	−1.88	1.54	2.43
YNTS	24.8617	121.7789	0.54 ± 0.04	0.58 ± 0.04	0.79 ± 0.06	0.49	−0.24	0.54

Table 4. Parameters of fault model.

	Middle top point Lon (°)	Lat (°)	Depth (km)	Strike (°)	Dip (°)	Length (km)	Width (km)	Strike-slip (mm)	Dip-slip (mm)	Tensile Slip (mm)	M_w_DC	$M_w\_non\text{-}DC$
S-M	121.800	24.665	1	75	85	15	12	37	−18	−27	5.50	5.48
GPS								79	−3	−58	5.69	5.70
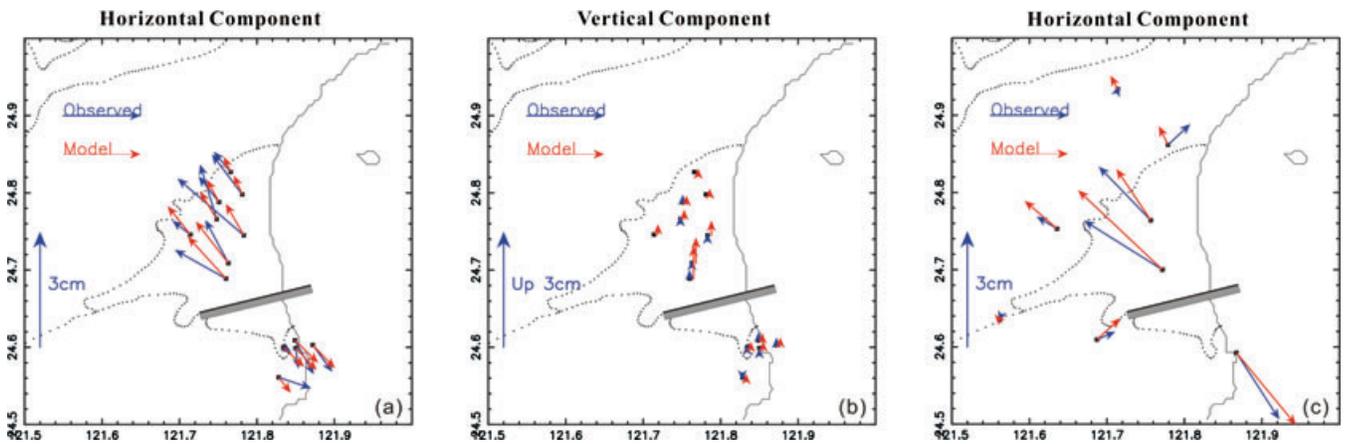
Figure 5. Maps show the coseismic displacements from the strong-motion records for both (a) the horizontal and (b) the vertical components, and (c) show the coseismic displacements from the daily solution GPS data for the horizontal component. The grey square is the projection of the modelled fault-plane and the thick black line is the top of it (see parameters of fault model in Table 4). The arrows show the displacements, including the modelled (red) and observed (blue).

(1985). Incorporated together is grid search to find the best-fitting fault model by way of iteration of calculating the values and directions of the coseismic displacements. The initial position and the area of the fault plane are constrained by the aftershock distribution (Fig. 2) and the different slip components are estimated by grid search. The parameters of final best-fitting fault model show significant tensile-slip and similar moment tensor of tensile faulting to shear faulting, indicating the tensile faulting indeed involved in this event (Table 4). The modelled slip is well matched except for the vertical components of some sites located in the northern side of the fault where is covered by thicker sediments than in the southern side, and the best-fitting double-couple (shear faulting) moment tensor is reasonable as well (Figs 5a and b; Table 4). Separately, we also obtained the best-fitting fault model inverted from the GPS data with the same fault geometry, showing the amounts of tensile and shear slips are slightly more than double of the first main shock, which are the sum of two coseismic slips and their post-seismic

slips within one day (Fig. 5c; Table 4). It infers the first and second main shocks probably produce the corresponding coseismic slips.

6 DISCUSSION

6.1 The possible faulting behaviour of the second main shock

Except for the broken station and weak signals, the main problem of coseismic displacement determination is the poor signal with big standard error, which may be caused by the sustained short period surface wave vibration in the soft sediments. With enough time for attenuation we still can determine the final permanent displacement; however, the second main shock occurred only 68 seconds later hardly make the precise determination. Also, the sustained surface wave vibration induced from the first main shock let the coseismic

displacement determination of the second shock become almost impossible. By comparison with the daily GPS result, which is the combination of the coseismic displacements from the earthquake doublet and part of their post-seismic displacements, the coseismic displacement result of our first main shock presents the similar slip direction but only half amounts of displacements (Fig. 4; Tables 2 and 3). It infers that the second main shock produced same deformation including the horizontal and vertical components, further implying a similar focal mechanism, complex faulting integrated tensile faulting with shear faulting.

6.2 The source mechanism of seismogenic structure underneath the Ilan Plain

The focal mechanisms of the two main shocks are classified as normal type by using dense strong motion records with the first motion method while the CMT solutions show dominated strike-slip motion by waveform inversion method. It has been suggested that the rupture underwent an initial normal motion followed by a strike-slip by the study on the spatial slip distributions of the 2005 event derived from finite fault model (Tsao 2006). Similar conclusion has been given as that the main shock was driven by normal faulting at first representing the initial down-slip rupture and later changed to left-lateral strike-slip motion representing the average rupture by analysis of near-field waveform inversion (Wang 2007). However, our result of coseismic displacement shows the blocks in both sides of the seismic cluster moved with high angle to the cluster at the same time in similar centimetre-scale but opposite direction, and negligible vertical movements. Neither normal faulting nor strike-slip faulting can satisfy such observation of coseismic ground displacements. Furthermore, the dislocation model shows the slip vectors are dominated by strike-slip and tensile-slip faulting and not constrained to lie on the fault plane, elucidating possible occurrence of tensile deformation. We suggested that the normal faulting with first motion method is due to the tensile deformation while the rest of the strike-slip component corresponds to CMT solution; hence the discrepancy in the focal mechanisms is not caused by the changes of the rake of the slip but by tensile faulting. Also, near-field waveform inversion obtained large (∼27 per cent) compensated linear vector dipole (CLVD) component in strike-slip CMT solution (Wang 2007) as well as Harvard CMT solution. Those phenomena indicate this earthquake doublet is not a well double-couple event, but a non-double-couple event instead.

Non-double-couple events have been discovered in many different environments inclusive of landslides, volcanic and geothermal areas, mines, and deep subduction zones. Shallow earthquakes in volcanic or geothermal areas and mines often have mechanisms consistent with failure involving both tensile and shear faulting, which may be facilitated by high-pressure and/or high-temperature fluids
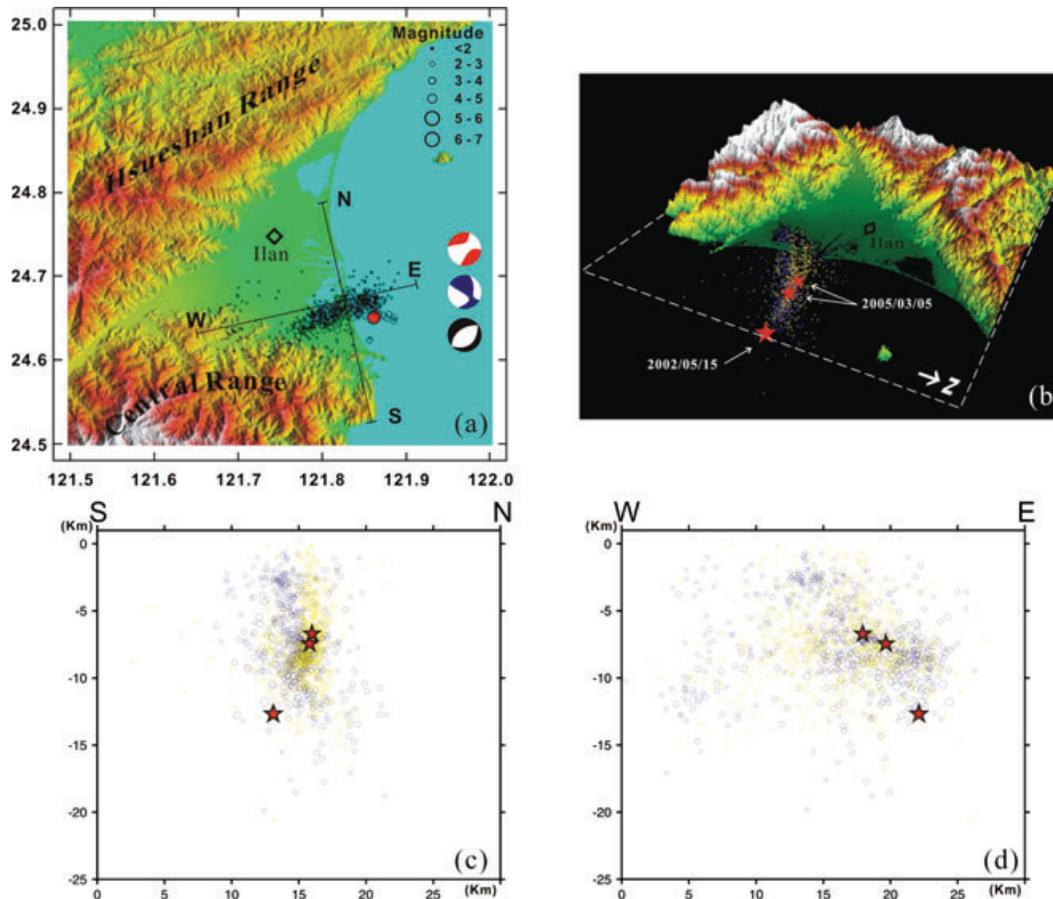
Figure 6. (a) The distribution of relocated epicentres of the main shock and associated aftershocks of the 2002 Ilan earthquake in northeastern Taiwan (see location in Fig. 1b). (b) Perspective view of the similar seismic clusters, and (c) N–S and (d) E–W cross-sections of projected hypocentres of 2002 (in blue) and 2005 (in yellow) events underneath Ilan Plain show the propagating main shocks (V.E. 3× in topography). Red asterisks show the hypocentres of the main shocks.

with CLVD mechanism (Julian *et al.* 1998; Miller *et al.* 1998). There are active volcanoes and high geothermal activities in the surrounding Ilan area, especially the active volcanic island, the Kueishantao Island (Chen *et al.* 1995; Wang *et al.* 1999; Chung *et al.* 2000; Chen *et al.* 2001; see location in Fig. 1b), and the largest known productive geothermal area in Taiwan, the Chingshui geothermal area (Tseng 1978; Hsiao & Chiang 1979; Tong *et al.* 2008, see location in Fig. 1b). Geochemical study on gas and fluid implies that the mantle source may have invaded into Ilan Plain (Yang *et al.* 2005), while the tomographic study indicates the melting features beneath northeast Taiwan (Lin *et al.* 2004). We therefore supposed the 2005 earthquake doublet event is resulted from possible dyke intrusion which elucidating the mechanism of active backarc spreading of Okinawa Trough on opening Ilan Plain. To further verify the fluid source the advance geochemical and geophysical approaches are necessary.

6.3 Seismic crisis in Ilan area

In Ilan area the two normal fault systems on the north and south along the mountain front are assumed as the most possible active structures and potential sources of future earthquakes (Shyu *et al.* 2005b, Fig. 1b), while others may be hidden by thick sediments; however, no report could directly indicate any active faulting and associated earthquake in this area before. Several earthquake events in Ilan area show similar identities of the different focal mechanisms revealed by different determination methods as well as the 2005 earthquake doublet event (Wu *et al.* 2008c). The focal solution of 2002 ($M_L = 6.2$) event in Ilan area, for example, is determined as normal type by first-motion polarities, but strike-slip fault from Harvard and BATS CMT solutions (Wu *et al.* 2008c, Fig. 6). By using the same data source and relocation method applied to 2005 event, the epicentre of the 2002 event was located offshore at 24.652°N, 121.861°E with focal depth of 12.62 km only few kilometres away seaward to the 2005 event; moreover, the distribution of its aftershocks were almost coincided with the fault geometry from 2005 earthquake doublet event (Fig. 6). Therefore, we speculate the 2002 event was induced by the same seismogenic source as the 2005 event and this intrusion is probably propagating upward and landward in Ilan area (Fig. 6). Considering the seismic crisis in Ilan area, not only the post-collisional collapsing normal faults but the tensile source of propagating dyke intrusion associated with the active spreading Okinawa Trough will generate earthquake with magnitude more than six and cause damages in this populated area.

7 CONCLUSION

2005 Ilan earthquake doublet event provided an excellent chance to unravel the mystery beneath the fast sediment accumulation area, Ilan Plain. Our results first verified the existence of a seismogenic fault which generated the 2005 event with significant component of tensile source underneath the Ilan Plain based on analysis of aftershocks cluster, coseismic displacements from daily solution GPS and from strong-motion records of the 2005 event, and inverted dislocation model. Furthermore we also demonstrated the two main shocks with similar behaviour produced the same deformation.

The large CLVD mechanism of the event involving both tensile and shear faulting indicates the fluid effect; while other geochemical and geophysical inferred mantle source and melting features underneath the Ilan Plain. We therefore interpret the 2005 Ilan earthquake

doublet event is resulted from the dyke intrusion at the southwestern tip of the Okinawa Trough, which is reasonably driven by active backarc spreading.

The features of focal mechanism and fault geometry of the previous 2002 event in study area are much similar with 2005 event; hence we suppose the 2002 event was also resulted from the dyke intrusion. Moreover, the former 2002 event took place deeper and farther east than 2005 event. We interpret the dyke intrusion is probably propagating upward and landward resulting in the future seismic crisis in Ilan area as well as the post-collisional collapsing normal fault systems.

REFERENCES

Boore, D.M., 2001. Effect of baseline corrections on displacement and response spectra for several recodings of the 1999 Chi-Chi Earthquake, Taiwan, *Bull. seism. Soc. Am.,* **91,** 1199–1211.

Boore, D.M., Stephens, C.D. & Joyner, W.B., 2002. Comments on baseline correction of digital strong-motion data: examples from the 1999 Hector Mine, California, earthquake, *Bull. seism. Soc. Am.,* **92,** 1543–1560.

Chen, C.H., Lee, T., Shieh, Y.N., Chen, C.H. & Hsu, W.Y., 1995. Magmatism at the onset of back-arc basin spreading in the Okinawa Trough, *J. Volcanol. Geother. Res.,* **69,** 313–322.

Chen, Y.G., Wu, W.S., Chen, C.H. & Liu, T.K., 2001. A date for volcanic eruption inferred from a siltstone xenolith, *Quater. Sci. Rev.,* **20,** 869–873.

Chiang, S.C., 1976. Seismic prospecting in the Ilan Plain, *Miner. Technol.,* **14,** 215–221. (In Chinese)

Chiu, H.C., 1997. Stable baseline correction of digital strong-motion data, *Bull. seism. Soc. Am.,* **87,** 932–944.

Chung, S.L., Wang, S.L., Shinjo, R., Lee, C.S. & Chen, C.H., 2000. Initiation of arc magmatism in an embryonic continental rifting zone of the southernmost part of Okinawa Trough, *Terra Nova,* **12,** 225–230.

Davis, S.D. & Frohlich, C., 1991. Single-link cluster analysis of earthquake aftershocks: decay laws and regional variations, *J. geophys. Res.,* **96,** 6336–6350.

Ho, C.S., 1986. A synthesis of the geologic evolution of Taiwan. *Tectonophysics,* **125,** 1–16.

Ho, C.S., 1988. *An Introduction to the Geology of Taiwan. Explanatory Text of the Geologic Map of Taiwan,* 2nd edn, Central Geological Survey, Taipei, 192 pp.

Ho, C.S., 2007. *Monitoring of Active Structures related Crustal Deformation in Taiwan* (in Chinese with English abstract), *PhD thesis.* National Taiwan University, Taipei, Taiwan, 209 pp.

Hsiao, P.T. & Chiang, S.C., 1979. Geology and geothermal system of the Chingshui-Tuchang geothermal area, Ilan, Taiwan, *Petrol. Geol. Taiwan,* **16,** 205–213.

Hsu, S.K., Sibuet, J.C. & Shyu, C.T., 1996. High-resolution detection of geologic boundaries from potential-field anomalies: An enhanced analytic signal technique, *Geophysics,* **61,** 373–386.

Hsu, Y.J., 1999. *GPS investigation of extension in the Ilan Plain* (in Chinese with English abstract), *MS thesis.* National Central University, Chungli, Taiwan, 108 pp.

Iwan, W.D., Moser, M.A. & Peng, C.Y., 1985. Some observations on strong-motion earthquake measurement using a digital accelerograph, *Bul. seism. Soc. Am.,* **75,** 1225–1246.

Julian, B.R., Miller, A.D. & Foulger, G.R., 1998. Non-double-couple earthquakes 1. Theory, *Rev. Geophys.,* **36**(4), 525–549.

Lee, C.T. & Wang, Y., 1988. Quaternary stress changes in northern Taiwan and their tectonic significance, *Geol. Soc. China Proc.,* **31,** 154–168.

Letouzey, J. & Kimura, M., 1986. The Okinawa Trough: Genesis of a back-arc basin developing along a continental margin, *Tectonophysics,* **125,** 209–230.

Lin, J.Y., Hsu, S.K. & Sibuet, J.C., 2004. Melting features along the western Ryukyu slab edge (northeast Taiwan): tomographic evidence, *J. geophys. Res.,* **109,** B12402, doi:10.1029/2004JB003260.

Liu, C.C., 1995. The Ilan Plain and the southwestward extending Okinawa Trough, *J. Geol. Soc. China,* **38,** 111–119.

Miller, A.D., Foulger, G.R. & Julian, B.R., 1998. Non-double-couple earthquakes 2. Oberservations, *Rev. Geophys.,* **36**(4), 551–568.

Okada, Y., 1985. Surface deformation due to shear and tensile faults in a half-space, *Bull. sseism. Soc. Am.,* **75,** 1135–1154.

Sheu, H.C., 1987. Crustal deformation of the southern tip of Okinawa Trough and Ilan area, Taiwan, *Measurement Engineering,* **29**(3), 1–6 (in Chinese).

Shin, T.C., Tsai, Y.B., Yeh, Y.T., Liu, C.C. & Wu, Y.M., 2003. Strong-Motion Instrumentation Programs in Taiwan, in *Handbook of Earthquake and Engineering Seismology,* pp. 1057–1602, eds Lee, W.H.K., Kanamori, H. & Jennings, P.C., Academic Press, San Diego, CA.

Shyu, J.B.H., Sieh, K. & Chen, Y.G, 2005a. Tandem suturing and disarticulation of the Taiwan orogen revealed by its neotectonic elements, *Earth planet. Sci. Lett.,* **233,** 167–177.

Shyu, J.B.H., Sieh, K., Chen, Y.G. & Liu, C.S., 2005b. Neotectonic architecture of Taiwan and its implications for future large earthquakes, *J. geophys. Res.,* **110,** B08402, doi:10.1029/2004JB003251.

Sibuet, J.C., Deffontaines, B., Hsu, S.K., Thareau, N., Formal, J.P.L., Liu, C.S. & Party, A., 1998. Okinawa trough backarc basin: Early tectonic and magmatic evolution, *J. geophys. Res.,* **103,** 30 245–30 267.

Suppe, J., 1984. Kinematics of arc-continent collision, flipping of subduction, and back-arc spreading near Taiwan, *Memoir Geol. Soc. China,* **6,** 21–33.

Teng, L.S., 1990. Late Cenozoic arc-continent collision in Taiwan, *Tectonophysics,* **183,** 57–76.

Teng, L.S., 1996. Extensional collapse of the northern Taiwan mountain belt, *Geology,* **24,** 949–952.

Thurber, C.H. & Eberhart-Phillips, D., 1999. Local earthquake tomography with flexible gridding, *Comput. Geosci.,* **25,** 809–818.

Tong, L.T., Ouyang, S., Guo, T.R., Lee, C.R., Hu, K.H., Lee, C.L. & Wang, C.J., 2008. Insight into the geothermal structure in Chingshui, Ilan, Taiwan, *Terr. Atmos. Ocean. Sci.,* **19,** 413–424, doi:10.3319/TAO.2008.19.4.413(T).

Tsai, Y.B., Feng, C.C., Chiu, J.M. & Liaw, H.B., 1975. Correlation between micro-earthquakes and geologic faults in the Hsintien-Ilan area, *Petrol. Geol. Taiwan,* **12,** 149–167.

Tsao, C.W., 2006. *Slip distributions of 2005 earthquake doublet beneath I-Lan plain, Taiwan* (in Chinese with English abstract), *Master thesis*. National Central University, Chungli, Taiwan, 83 pp.

Tseng, C.S., 1978. Geology and geothermal occurrence of the Chingshui and Tuchang districts, Ilan, *Petrol. Geol. Taiwan,* **15,** 11–23.

Wang, K.L., Chung, S.L., Chen, C.H., Shinjo, R., Yang, T.F. & Chen, C.H., 1999. Post-collisional magmatism around northern Taiwan and its relation with opening of the Okinawa Trough, *Tectonophysics,* **308,** 363–376.

Wang, T.H., 2007. The Ilan earthquake pair on 5 March 2005: Discussion on focal mechanism determination with near-field waveform inversion, *Master thesis*. National Taiwan University, Taipei, Taiwan, 79 pp.

Wu, Y.M. & Chen, C.C., 2007. Seismic reversal pattern for the 1999 Chi-Chi, Taiwan, Mw 7.6 earthquake, *Tectonophysics,* **429,** 125–132.

Wu, Y.M. & Chiao, L.Y., 2006. Seismic quiescence before the 1999 Chi-Chi, Taiwan Mw7.6 earthquake, *Bull. seism. Soc. Am.,* **96,** 321–327.

Wu, Y.M. & Wu, C.F., 2007. Approximate recovery of coseismic deformation from Taiwan strong-motion records, *J. Seism.,* **11,** 159–170, doi:10.1007/s10950–006-9043-x.

Wu, Y.M., Chang, C.H., Hiao, N.C. & Wu, F.T., 2003. Relocation of the 1998 Rueyli Taiwan, earthquake sequence using three-dimensions velocity structure with stations corrections, *Terres. Atmos. Ocean. Sci.,* **14,** 421–430.

Wu, Y.M., Chen, Y.G., Chang, C.H., Chung, L.H., Teng, T.L., Wu, F.T. & Wu, C.F., 2006a. Seismogenic structure in a tectonic suture zone: with new constraints from 2006 Mw6.1 Taitung earthquake, *Geophys. Res. Lett.,* **33,** L22305.

Wu, Y.M., Chen, Y.G., Shin, T.C., Kuochen, H., Hou, C.S., Chang, C.H., Wu, C.F. & Teng, T.L., 2006b. Coseismic vs. interseismic ground deformations, faults rupture inversion and segmentation revealed by 2003 Mw 6.8 Chengkung earthquake in eastern Taiwan, *Geophys. Res. Lett.,* **33,** L02312.

Wu, Y.M., Chang, C.H., Zhao, L., Shyu, J.B.H., Chen, Y.G., Sieh, K. & Avouac, J.-P., 2007. Seismic Tomography of Taiwan: improved constraints from a dense network of strong-motion records, *J. geophys. Res.,* **112,** B08312, doi:10.1029/2007JB004983.

Wu, Y.M., Chang, C.H., Zhao, L., Teng, T.L. & Nakamura, M., 2008a. A comprehensive relocation of earthquakes in Taiwan from 1991 to 2005, *Bull. seism. Soc. Am.,* **98,** 1471–1481, doi:10.1785/0120070166.

Wu, Y.M., Chen, C.C., Zhao, L. & Chang, C.H., 2008b. Seismicity characteristics before the 2003 Chengkung, Taiwan Mw6.8 earthquake, *Tectonophysics,* **457,** 177–182, doi:10.1016/j.tecto.2008.06.007.

Wu, Y.M., Zhao, L., Chang, C.H. & Hsu, Y.J., 2008c. Focal-mechanism in Taiwan by genetic algorithm, *Bull. seism. Soc. Am.,* **98,** 651–661.

Yang, T.F. *et al.*, 2005. Gas compositions and helium isotopic ratios of fluid samples around Kueishantao, NE offshore Taiwan and its tectonic implications, *Geochem. J.,* **39,** 469–480.

Yeh, Y.H., Lin, C.H. & Roecker, S.W., 1989. A study of upper crustal structures beneath northeastern Taiwan: possible evidence of the western extension of Okinawa trough. *Proc. Geol. Soc. China,* **32,** 139–156.

Yu, S.B. & Tsai, Y.B., 1979. Geomagnetic anomalies of the Ilan Plain, Taiwan, *Petrol. Geol. Taiwan,* **16,** 19–27.

Yu, S.B., Chen, H.Y. & Kuo, L.C., 1997. Velocity field of GPS station in the Taiwan area, *Tectonophysics,* **274,** 41–59.